Detonation Initiation by Shock Focusing

E. Wintenberger, H. Hornung and J.E. Shepherd

Graduate Aeronautical Laboratories
California Institute of Technology
Pasadena, CA 91125

GALCIT Report FM2001.00X

2001, Revised December 27, 2021

This report was drafted in 2000-2001 as part of a preliminary investigation of the application of shock focusing to detonation initiation. EW and JES performed the literature survey. HH set up and guided the Amrita simulations by EW. The report was revised by JES and made publically available in 2021. This work provided motivation and background for the experimental and numerical study carried out by Pawel Buraczewski and published as GALCIT Report FM 2004.004.

Abstract

The focusing of shock waves by reflection from curved surfaces is investigated as a means of detonation initiation. Previous work on shock reflection and focusing is reviewed. Numerical simulations, solving the Euler equations for a non-reactive mixture in the two-dimensional (planar) case, have been carried out for planar parabolic reflectors varying the incident shock wave Mach number and the depth of the reflector. The results are expressed in the form of a diagram showing what type of reflection occurs as a function of these parameters. Pressure amplifications studies show that the highest amplification is obtained for type C reflections. This corresponds to a small triangular region of fluid being compressed between the two merging triple points and the reflected shock. Temperature contours were examined for different configurations in order to determine the size of the region of fluid above a relevant critical temperature for detonation initiation.

1 Introduction

Shock focusing creates zones of very high pressure and temperature which are obviously very favourable to detonation initiation. Shock focusing occurs (Fig. 1) when the two triple points formed at the intersection of the reflected shock and the shocks diffracted by the reflector corners intersect on the axis.

Three types of reflections have been observed at shock focusing for parabolic reflectors, depending on the strength of the incident shock wave and the depth of the reflector. Type A reflection corresponds to a strong shock and a shallow reflector, and is characterized by the formation of a Mach stem growing with time, leaving an open focal region. Type B reflection occurs when the shocks diffracted by the reflector edges intersect on the axis after

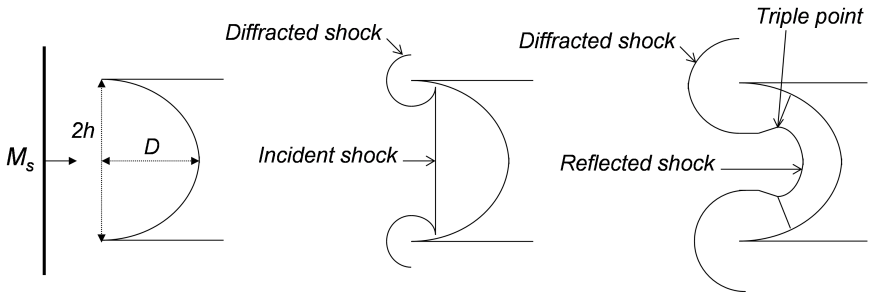

Figure 1: Schematic of focusing event.

focusing. Type C reflection, which occurs for weak shocks and deep reflectors, corresponds to the diffracted shocks intersecting before focusing and results in a closed focal region.

The initiation of a self-sustaining detonation wave requires a high amount of energy to be released in a large enough zone so that the necessary coupling between the leading shock front and the reaction zone can be triggered. There are two main ways to achieve detonation initiation: one is by directly initiating the detonation, the other is through deflagration-to-detonation transition (DDT). Direct initiation occurs when a sufficiently large amount of energy is released in a small region of unconfined combustible gas mixture. A strong spherical blast wave is created and expands while decaying. If the initial energy release is high enough, the blast wave velocity will decay to a constant value near the Chapman-Jouguet (CJ) detonation propagation velocity. If the initial energy release is too low, the blast wave decelerates below the CJ velocity as the reaction zone decouples from the shock front. Deflagration-to-detonation transition is the other mechanism for initiation of detonation. A low energy deposition creates a flame, which propagates at a typical velocity of a few m/s. This flame can be accelerated through its interaction with expanding shocked reactants, which cause compression waves that coalesce in shock waves ahead of the flame, its interaction with reflected shocks, which stretch and distort the flame, as well as with solid obstacles, which induce large-scale turbulence. Once the flame is accelerated, formation of explosion centers can occur as pockets of reactants reach critical ignition conditions. These explosion centers, or "hot spots", create small blast waves that amplify and merge into a self-sustaining detonation wave.

The interest towards DDT has been motivated by the difference in terms of initiation energy between direct initiation and DDT. Directly initiating a detonation typically requires an energy five or six orders of magnitude higher than the energy required to initiate a flame. This makes DDT initiation much more applicable to practical devices, such as pulse detonation engines. One of the critical steps in the occurrence of DDT is the formation of these hot spots, which are characterized by a very high pressure and temperature. They are usually formed by the interaction and merging of reflected shocks off the tube walls or the obstacles present in the tube. This phenomenon where shock waves merge into a small region and thus create a high pressure and temperature is referred to as shock focusing. It happens in a similar way when an incident planar shock wave is reflected from a concave reflector and converges towards the focus of the reflector cavity. The elevated pressure and temperature conditions are obviously very favourable in a combustible mixture to detonation initiation.

2 Shock focusing in non-reactive medium

Before considering the case of a reactive medium, where timescales associated with combustion processes play a role, it is useful to consider the case of shock focusing in an inert medium, where the only timescales involved are those associated with the gasdynamic flow.

2.1 Shock focusing flow field pattern

A pioneering study of shock focusing was the one of Sturtevant and Kulkarny (1976). They studied the focusing of weak shock waves after reflection from parabolic and cylindrical reflectors. They investigated the effect of the incident shock strength on the focusing pattern and isolated 3 different regimes. For an incident weak shock, the reflected shock comes out of the focus with a crossed and folded configuration. The diffracted shocks from the corners of the reflector cross in front and thus precede the focused shock, which follows between the folds. The focal region is limited to a single point for an acoustic wave, but extends to a small closed region if the shock is a bit stronger (cases a) and b) on Figure 2). In the case of moderately strong shocks, the focal region starts to open up. The three-shock intersections (triple points) cross once, producing the focusing effect, then turn around and come very close to a second crossing, but then move away. This is a delimiting case: if the incident shock strength is smaller, the triple points cross twice (case b)). For strong shocks, the focal spot never closes as the triple points simply move apart after focusing. The wave configuration is therefore not crossed and folded, but is flattened because of the flat Mach stem between the diverging triple points.

Izumi et al. (1994) carried out some experimental and numerical studies of the focusing process of shock waves reflected from various shapes of a parabolic reflector. They also investigated the effect of the incident shock strength. They proposed a classification of the patterns of shock wave focusing depending on the shock strength and the reflector depth (see Figure 3). Type A is characterized by diffracted shocks never intersecting before and after focusing. The reflected shock in the center grows, leaving the focal region open. The type of reflection obtained between the two diffracted waves is a Mach reflection. This case can be identified with the case d) described by Sturtevant and Kulkarny (1976), which is corroborated by the fact that Izumi et al. (1994) observed it for high incident Mach numbers and shallow reflector shapes. Type B focusing occurs when the diffracted shock waves from the corners of the reflector do not intersect each other before focusing but intersect after focusing. Finally, type C corresponds to the intersection of the diffracted waves before and after focusing (case b) of Sturtevant and Kulkarny (1976)). A triangular region is formed which is surrounded by the reflected wave coming from the center of the reflector and the diffracted waves coming from the sides. This region disappears at focusing, when the triple points behind it merge on the axis of the reflector. This focusing pattern was noticed to appear for weak incident shocks and deep reflectors. Types B and C correspond to a regular reflection pattern between the two diffracted waves.

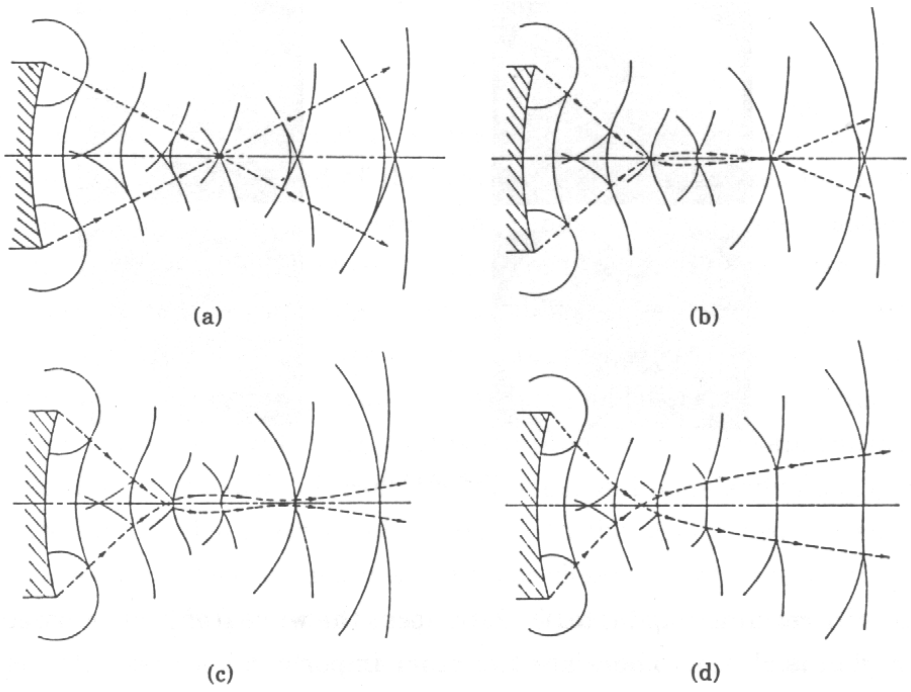

Figure 2: Schematic representation of the effect of shock strength on focusing. Perfect focus of: *a*) acoutic waves; *b*) weak shocks; *c*) moderately strong shocks; *d*) strong shocks. Figure reproduced from Sturtevant and Kulkarny (1976)

2.2 Mechanisms of shock focusing

As Milton (1989) pointed out, there are two types of focusing that need to be distinguished. The first one is free field focusing, in which case the reflected waves get focused to a point away from the reflector surface. The flow field patterns correspond to the ones previously described. The second type of focusing is the creation of an implosion by focusing the incoming wave to a line or a point along the reflector surface (depending on the case being two- or three-dimensional). This creates a cylindrical or spherical implosion, which is of course characterized by very high pressures and temperatures.

An example of free field shock focusing is the experiment of Perry and Kantrowitz (1951) where they generated converging cylindrical waves focusing on a line by using an inverted teardrop insert in a circular cross-section shock tube. In the case of free field focusing by reflection of an incident shock wave on a concave reflector, the incident shock reflects and interacts with the diffracted shocks from the reflector corners. This interaction creates a third shock behind the reflected shock along the reflector edges. This third shock is a Mach stem and triple points are created on either side of the reflector axis. These triple points move towards the central axis as the diffracted shocks expand. Their merging on the axis creates a region of very high pressure and temperature. This represents the shock focusing process and the point where the maximum pressure is obtained is referred to as the gasdynamic focus. This free field shock focusing process, due to the collision of two triple points on the center axis and independent of the reflector shape, was discovered by Sturtevant and

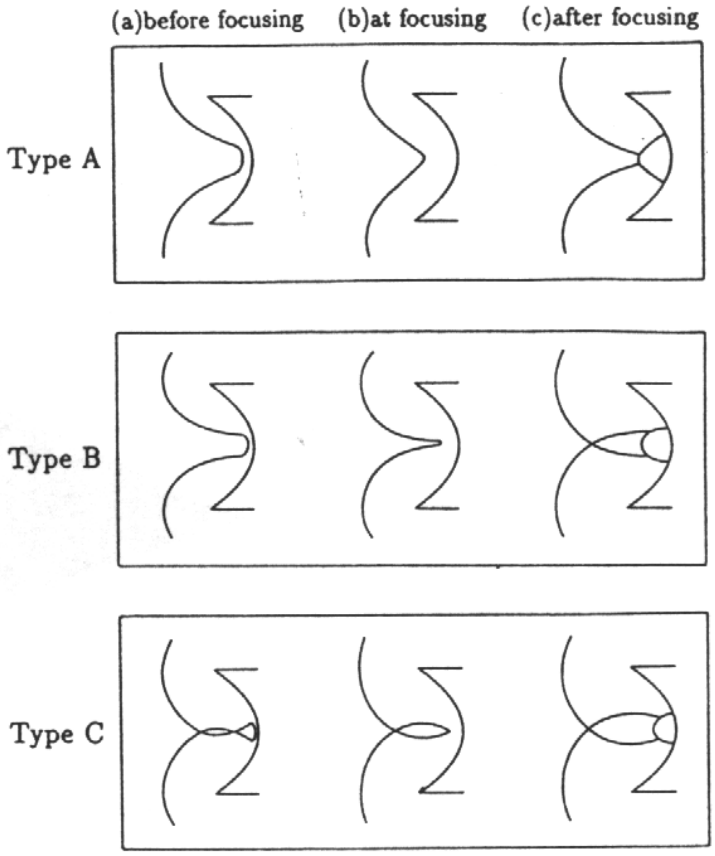

Figure 3: Different reflection types according to Izumi et al.. Figure reproduced from Izumi et al. (1994).

Kulkarny (1976). They also proved that the gasdynamic focus corresponds to the merging point of the two triple points. This mechanism was verified later by Izumi et al. (1994). The strong shock in the focal region is always followed by a sharp expansion, which brings the pressure down immediately after the wave has passed the gasdynamic focus. This expansion arises from the combination of the two expansion waves diffracted from the corners of the reflector.

The creation of an implosion implies the reduction of the shock front to a line in the two-dimensional case or a point in the three-dimensional case. It can be generated in a rectangular shock tube using a wall contraction. Based on the idea that maximization of the pressure and volume of high pressure at a point requires the suppression of reflected shock during implosion, Milton (1989) designed a logarithmic spiral. By centering the ray-shock characteristics at a point on the wall, which prevented Mach reflection, he was able to create an imploding shock wave. No reflected shocks were created before implosion. After implosion, a single, strong shock moves outwards. This configuration was compared to radiused ramp and parabola configurations, and pressure measurements showed that the logarithmic spiral produced much higher overpressures. The numerical work of Liang et al. (1999) also proved the existence of an implosion phenomenon for paraboloidal reflectors.

Extremely large pressure and temperature enhancement was observed.

2.3 Free field shock focusing

2.3.1 Maximum pressure at shock focusing

The maximum observed pressure occurs on the axis of symmetry, by definition at the gas-dynamic focus. Sturtevant and Kulkarny (1976) showed in the case of weak waves that the pressure outside the focal region was close to the predictions of geometrical acoustics. However, inside the focal region, the pressure does not become infinite as predicted by geometrical acoustics, but remains finite because of non-linear diffraction. Sturtevant (1989) explained the limitation of the amplitude at focus with the strong expansion waves following and overtaking the diffracted shocks at focus. The amplification of the pressure is usually expressed in terms of an amplification factor, defined as the ratio of the maximum pressure obtained to the reflected pressure for normal reflection. Sturtevant and Kulkarny (1976) obtained in their experiments amplification factors between 2 and 5 depending on the incident Mach number, the amplification decreasing for higher Mach numbers. These results were confirmed by the numerical simulations of Kishige et al. (1991) with parabolic reflectors, who found a high amplification factor for weak waves (up to 3), decreasing as the shock got stronger to asymptote around a value of 2. However, earlier numerical simulations by Nishida et al. (1986) and Nishida (1989) had failed to capture the experimentally observed behavior for weak shock waves, as the predicted amplification factor was getting close to 1 as the shock strength decreased. It was then increasing with increasing shock Mach number, before asymptoting at a value of the order of 2, depending on the reflector depth. More recent computations by Liang et al. (1995) for parabolic reflectors showed the same variation of the amplification factor with incident shock Mach number. At high Mach numbers, the amplification factor asymptotes again to a value of about 2. In overall, if numerical simulations reproduce correctly the flowfield and the pressure behavior for strong incident Mach numbers ($M > 1.5$), they do not seem able yet to consistently predict the actual pressure amplification for weak shock waves. Three-dimensional shock focusing has been studied both experimentally and numerically. The experiments of Holl and Grönig (1983) about the focusing of weak blast waves after reflection from an ellipsoidal reflector confirmed the high amplification of weak shock waves. They obtained amplification factors as high as 40 to 60 for reflected shock Mach numbers close to 1.005 and a value of about 7 was obtained for a reflected shock Mach number of 1.1. Higher amplification factors than in the two-dimensional case are obtained because a point focus is created, instead of a line focus. The energy density at the focus is higher, resulting in increased overpressures. The numerical study of Kishige et al. (1991) reproduced the observed behavior of an axisymmetrically parabolic reflector, with a maximum predicted overpressure for very weak waves of about 10.

The reflector cavity shape has a strong influence on the shock focusing pattern and the resulting pressure amplification. Typically, the deeper the cavity, the higher the pressure amplification. The shock focusing pattern is always dictated by the competition between the reflector depth and the incident shock Mach number. Sturtevant and Kulkarny (1976) observed that the non-linear effects in the focusing of a shock wave were due to the competing effects of the convergence of the fronts from the side and the non-linear acceleration of the

shock on the centre-line, which basically depend on the latter parameters. If the reflector is shallow and the Mach number is sufficiently high, the diffracted shocks will not have time to intersect before or after focusing (type A reflection). On the other hand, if the reflector is deep and the incident Mach number low, then the diffracted shocks will intersect each other before and after focusing (type C reflection). In this case, a small triangular region is squeezed between the reflected shock and the two diffracted shocks that have already intersected. As these shocks move, this region gets smaller and smaller until focusing happens. Unlike the type A reflection where shock merging occurs more from the sides, the three merging shocks come from three opposite directions which enhances the compression of the focusing zone. The influence of the reflector depth on the pressure amplification was studied by the numerical work of Nishida et al. (1986) and Nishida (1989) who obtained pressure amplification factors from 1.3 to 3 for parabolic reflectors with increasing depth.

2.3.2 Gasdynamic focus location

The gasdynamic focus is defined as the locus of the point of maximum pressure, and does not correspond in general to the geometrical focus of the reflector. Weak shock waves tend to focus at the geometrical focus, as was shown by Holl and Grönig (1983) for weak blast waves. This idea was confirmed by the work of Nishida et al. (1986) and Nishida (1989). However, the numerical simulations also showed that as the Mach number increased, the gasdynamic focus shifted to lay between the reflector and the geometrical focus. For strong incident shocks, it tends to lay at a distance from the reflector of about 0.4 times the reflector focal distance. In addition, the locus of the gasdynamic focus varies with the reflector cavity depth, going away from the geometrical focus in the direction of the reflector as the reflector becomes shallow. The variation of the gasdynamic focus with the incident shock Mach number and the reflector depth are caused by the non-linear gasdynamic effects. In the case of weak shock waves, where non-linearity disappears, the gasdynamic focus is located at the geometrical focus.

2.3.3 Maximum temperature at shock focusing

From the point of view of detonation initiation, the location of the maximum temperature point is critical as temperature is usually the main triggering parameter for ignition. In the case of free field shock focusing, the maximum temperature was found to occur at the gasdynamic focus. The numerical results of Kishige et al. (1991) for shock focusing of a monoatomic gas (argon) using parabolic walls show that the maximum temperature was obtained at the same space-time location as the maximum pressure. The temperature ratios (maximum temperature over initial temperature) are very high (of the order of 10 for an incident Mach number of 3), but no real gas effects were considered in these cases. They confirmed qualitatively their results by experimentally measuring the radiation emission due to the ionization of argon in an axisymmetrically parabolic wall. Medvedev et al. (1995) observed the existence of a temperature maximum at shock focusing by measuring the heat radiation with a photodiode along the reflector axis. Values of the maximum temperature, dependent on the incident shock wave Mach number and the reflector shape, were obtained for conical and parabolic reflectors. The numerical study of Liang et al. (1995)

also showed that the location of the temperature maximum coincides with the gasdynamic focus. However, the temperature amplification (maximum temperature over temperature behind reflected shock) is lower than the pressure amplification: shock focusing accounted for a temperature increase of 24% on the normal reflection case. Kishige et al. (1991) found temperature increases of about 40% over the normal reflection case, but these results do not take into account real gas effects.

2.4 Implosion case

In the case of concave reflectors, implosion is caused when the diffracted waves interact with the incident shock wave to form two Mach stems that will merge with the incident shock wave at the reflector center. Similarly to what Milton (1989) observed, the implosion is characterized by a maximization of energy concentration on a point or a line. Liang et al. (1999) investigated this phenomenon and noticed that it happened for a given axisymmetric reflector shape and a range of incident shock Mach numbers. The pressure amplification obtained at the reflector center was extremely large, on the order of several hundreds for the axisymmetric case (point implosion) and of 5 for the two-dimensional case (line implosion). These values were obtained for incident shock Mach numbers varying between 1.2 and 2. Similarly, the temperature magnification was increased up to values of the order of 5 to 10 in the axisymmetric case and 2 in the two-dimensional case. In comparison, for free field focusing the values obtained for pressure amplification were around 2 and for temperature amplification around 1.25. After implosion, the reflected shock wave starts to focus, resulting in a second pressure peak. This pressure peak is lower than the peak at the reflector center. Implosion was found to occur in the case of a deep reflector at a lower Mach number than in the case of a shallow reflector. Liang et al. (1999) also noticed that the maximum temperature location could be different from the gasdynamic focus.

3 Numerical Simulation of Shock Focusing

Numerical simulations of shock wave reflection were performed using the AMRITA (Quirk, 1998) adpative mesh-refinement software to solve the Euler equations with the ideal gas (nonreactive) model ($\gamma = 1.4$). Planar shock waves followed by uniform flow were incident on two-dimensional (planar Carteian geometry) parabolic reflectors with varying values of the reflector depth-to-half-height ratio D/h and incident shock Mach number M_s.

The result were validated by comparison with the experiments of Izumi et al. (1994). Selected cases for the three reflection patterns (A, B, C) are shown in Fig. 4. The numerical simulations are in accord with the observations of Izumi et al. (1994). Type A reflection is characterized by the formation at focusing of a strong Mach stem growing with time. Type B reflection happens when the diffracted shocks at the reflector edges intersect on the axis after focusing and then precede the Mach stem. Type C reflection happens when the diffracted shocks at the reflector edges intersect on the axis before focusing. It results in a closed focal region. It is characterized by a small triangular region of fluid being compressed at focusing.

Examples of Amrita simulation results for two reflectors ($D/h = 0.75$ and 1.5) are shown as pressure and temperature contours in Fig. 5 for an incident shock Mach number of 2.0.

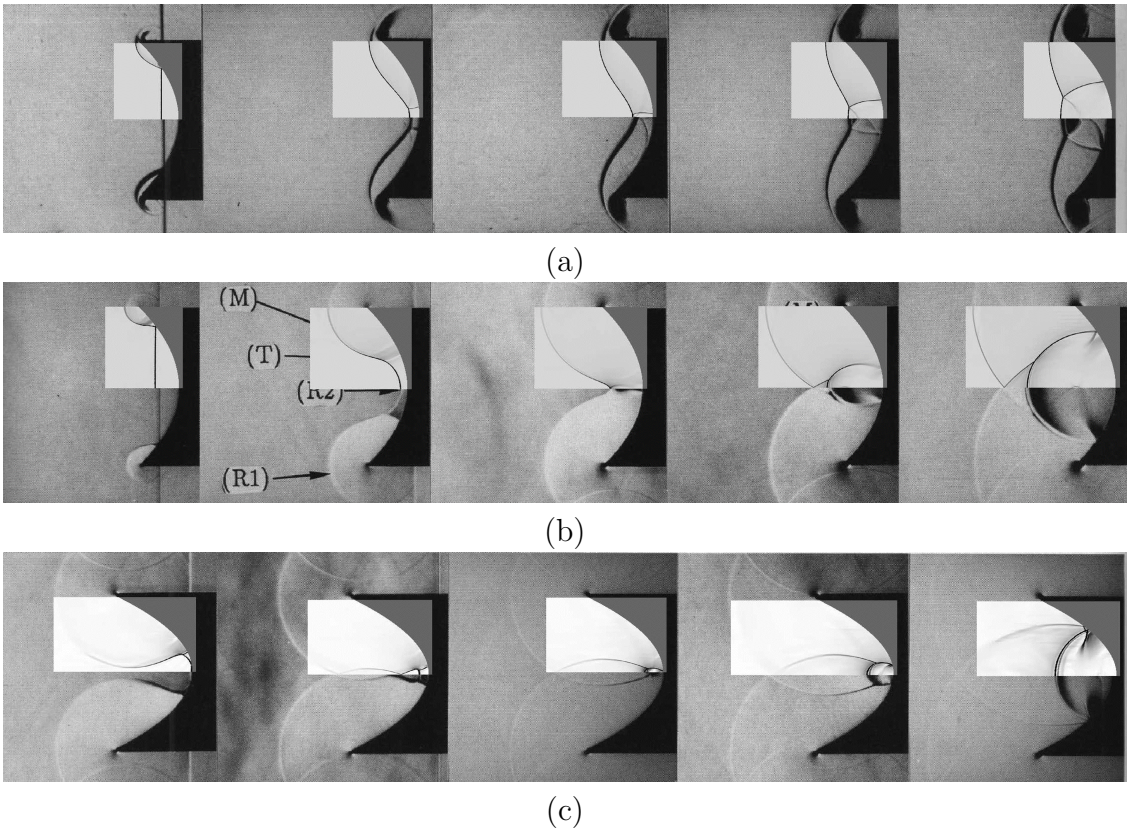

Figure 4: Comparison of Amrita simulation with selected cases investigated by Izumi et al. (1994). (a) Type A reflection, $M_s = 1.5$, $D/h = 0.5$. (b) Type B reflection, $M_s = 1.1$, $D/h = 0.5$. (b) Type C reflection, $M_s = 1.1$, $D/h = 1$.

The pressure and temperature spatial profiles along the reflector centerline are shown in Fig. 6. Peak pressures and temperatures are higher in type C than type A reflections but the pressure peak decays more rapidly due in type A than type C due to the stronger expansion wave following the reflected shock. The peak pressure in shock focusing may not accurately predicted near the focus in numerical simulations some features of the focus are singularities in the Euler equation model of gas dynamics. The peak values of quantities computed near these singular features will depend on the resolution of the numerical method. In addition, there are important physical and chemical processes in high-temperature gases which are not represented in the simple ideal gas model of the equation of state used in the present simulations.

The results of simulations for a range of reflector parameters ($0.4 \leq D/h \leq 1.8$) and incident shock Mach numbers ($1.1 \leq M_s \leq 3$) are given in Table 1 and summarized in Fig. 7 .

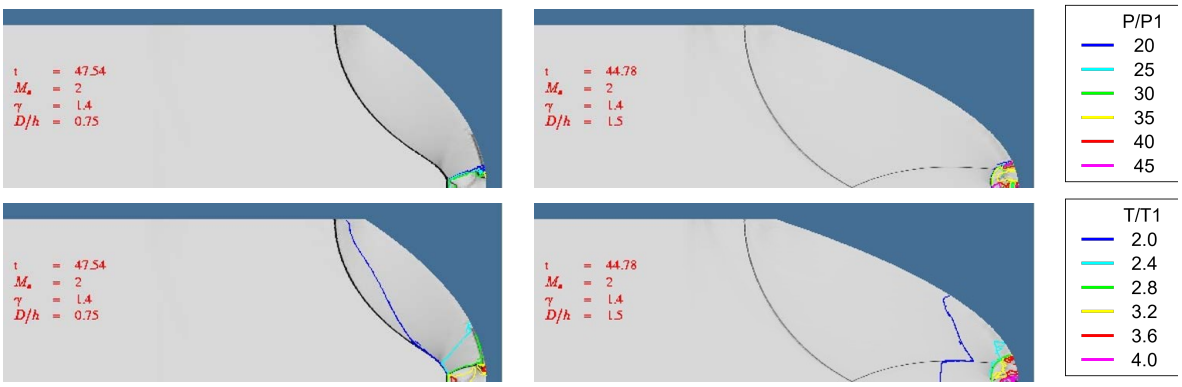

(a) (b)

Figure 5: Snapshots of pressure and temperature contours from of Amrita simulations of focusing events in two reflectors with $M_s = 2.0$. (a) Type A reflection pattern, $D/h = 0.75$. (b) Type C reflection pattern, $D/h = 1.5$

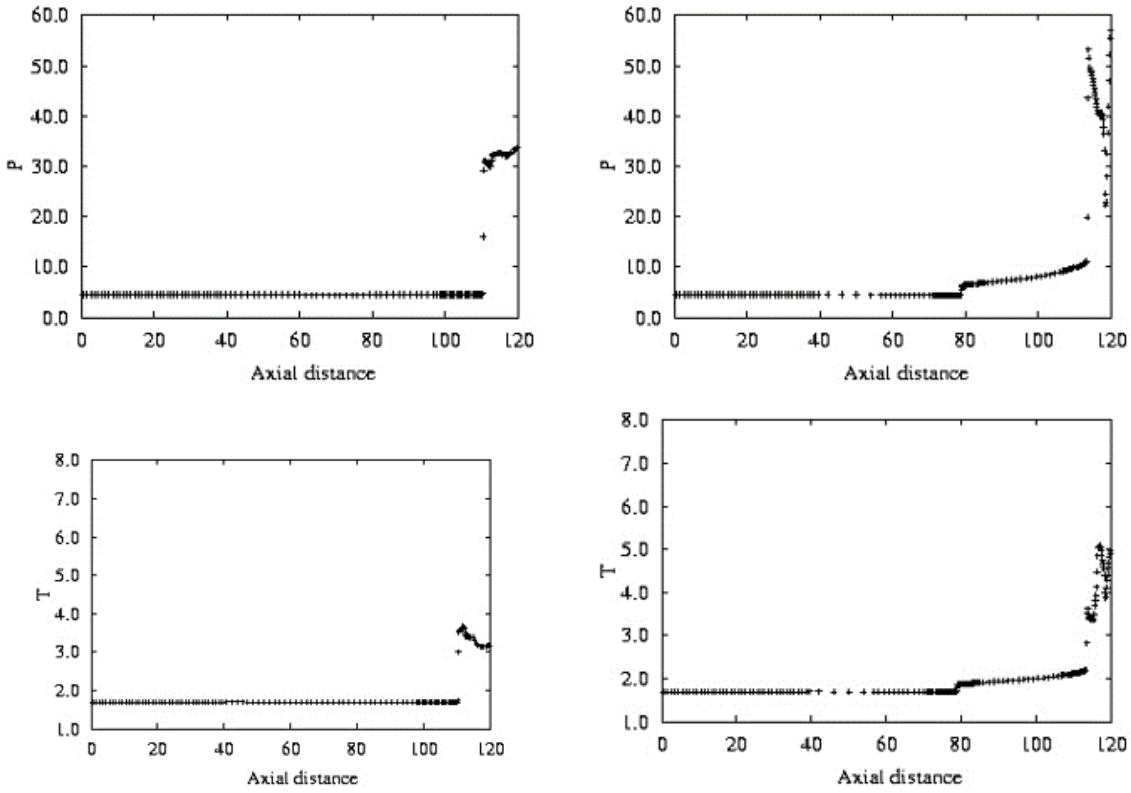

(a) (b)

Figure 6: Pressure and temperature profiles along the reflector centerline for the Amrita simulations of focusing events shown in Fig. 5. (a) Type A reflection pattern, $D/h = 0.75$. (b) Type C reflection pattern, $D/h = 1.5$

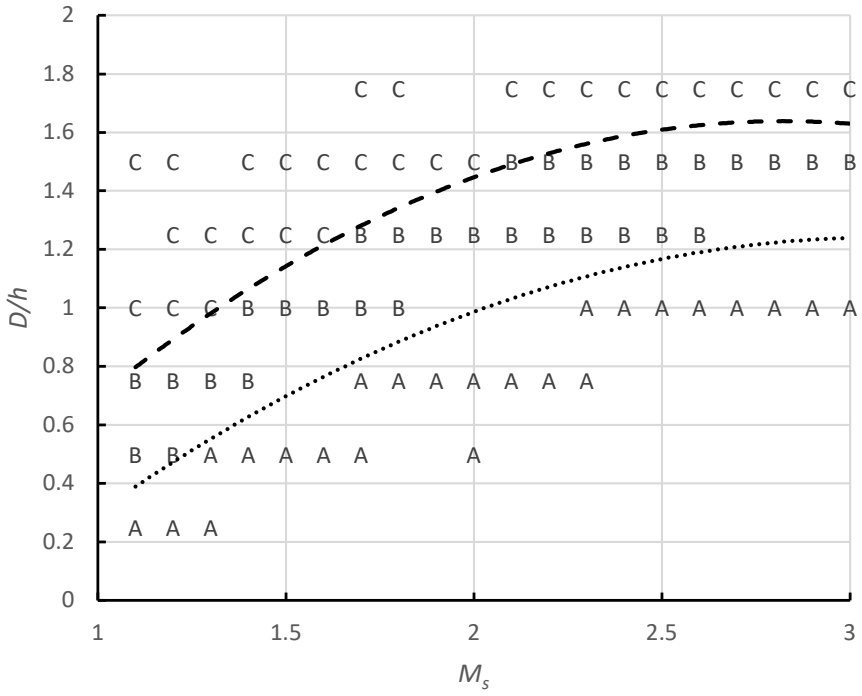

Figure 7: Reflection patterns for parabolic reflectors as a function of reflector depth ratio D/h and incident shock Mach number M_s.

Table 1: Reflection patterns observed in numerical simulations with two-dimensional (planar) parabolic reflectors

Type A		Type B		Type C	
M_s	D/h	M_s	D/h	M_s	D/h
1.1	0.25	1.1	0.5	1.1	1.0
1.2	0.25	1.1	0.75	1.1	1.5
1.3	0.25	1.2	0.5	1.2	1.0
1.3	0.5	1.2	0.75	1.2	1.25
1.4	0.5	1.3	0.75	1.2	1.5
1.5	0.5	1.4	0.75	1.3	1.0
1.6	0.5	1.4	1.0	1.3	1.25
1.7	0.5	1.5	1.0	1.4	1.25
1.7	0.75	1.6	1.0	1.4	1.5
1.8	0.75	1.7	1.0	1.5	1.25
1.9	0.75	1.7	1.25	1.5	1.5
2.0	0.5	1.8	1.0	1.6	1.25
2.0	0.75	1.8	1.25	1.6	1.5
2.1	0.75	1.9	1.25	1.7	1.5
2.2	0.75	2	1.25	1.7	1.75
2.3	0.75	2.1	1.25	1.8	1.5
2.3	1.0	2.1	1.5	1.8	1.75
2.4	1.0	2.2	1.25	1.9	1.5
2.5	1.0	2.2	1.5	2.0	1.5
2.6	1.0	2.3	1.25	2.1	1.75
2.7	1.0	2.3	1.5	2.2	1.75
2.8	1.0	2.4	1.25	2.3	1.75
2.9	1.0	2.4	1.5	2.4	1.75
3.0	1.0	2.5	1.25	2.5	1.75
		2.5	1.5	2.6	1.75
		2.6	1.25	2.7	1.75
		2.6	1.5	2.8	1.75
		2.7	1.5	2.9	1.75
		2.8	1.5	3	1.75
		2.9	1.5		
		3.0	1.5		

4 Shock focusing in a reactive medium

4.1 Relevance of shock focusing in the deflagration-to-detonation process

The onset of detonation by DDT is linked to the formation of regions of high pressure and temperature resulting from shock reflection off obstacles. These regions, or "kernels", depend on the strength of the leading shock ahead of the accelerated flame and on the type of reflection this shock will encounter. Chan (1995) studied the collision of shock waves with obstacles in a combustible mixture. The strength of the shock waves was set to values similar to those of shock waves formed ahead of accelerated flames (typically $M \simeq 2$). The mixture studied was hydrogen-oxygen and the obstacles were formed with baffles and wedge-baffle combinations. Ignition was observed to occur on the upstream side of the second obstacle due to the formation and reflection of a Mach stem along the wall, or on the upstream face of the first obstacle for a stronger shock wave. Ignition depended on the temperature created behind these reflected waves relative to the mixture autoignition temperature. The author pointed out the major role played by the local strengthening of the leading shock by shock diffraction and reflection. The gasdynamic mechanisms at the origin of ignition are the same as the ones observed in the case of shock focusing. Brown and Thomas (2000) carried out similar experiments that highlight the importance of two-dimensional multiple shock reflection and diffraction for transition to detonation. An incident shock wave on a rectangular obstacle was studied using inert and reactive mixtures including propane-air, propane-oxygen-argon and ethylene-oxygen-argon. Spark Schlieren photographs showed the onset of detonation. Initiation was observed to occur either behind the reflected shock on the upstream side of the obstacle, behind the diffracted shock above the obstacle after reflection on the top wall, or behind the diffracted shock wave at the downstream corner of the obstacle after it has reflected off the bottom wall. These experiments show how, for an initially weak shock, multiple reflections can cause at least pressure and temperature rises and possibly ignition. The authors emphasized the dependence of the events on the gas dynamics and the chemical kinetics of the mixture and pointed out the critical role played by the temperature.

4.2 Different regimes of ignition

Shock-induced ignition of a gaseous combustible mixture can occur in two main modes, depending on the thermodynamic conditions behind the shock wave. At lower temperatures, the ignition is referred to as mild, or weak. The gasdynamic explosion develops gradually. At higher temperatures, the ignition is referred to as strong or sharp. In this case, a secondary shock immediately appears which is followed by the reaction zone. Typical thermodynamic conditions for ignition are usually created using a reflected-shock tube technique, which is also very useful for measuring ignition delay times.

Strong ignition is characterized by the appearance of a steep and relatively flat pressure front, called the reaction shock, some time after the incident shock wave has reflected. This reaction shock is created very close to the wall by an explosion in the gas layer adjacent to the wall which triggered ignition in the gas throughout the entire cross-section of the tube. On the other hand, in the case of mild ignition, the reaction starts at some distinct centers,

usually in the stagnant regions at the corners. Flame fronts propagate slowly out of these explosion centers, before the onset of an "explosion in the explosion". The formation of this "explosion in the explosion" is associated with the convergence of flame fronts around a pocket of unburned mixture, which is compressed by this imploding flame-driven wave. The pressure rise generated by this "explosion in the explosion" may be sufficiently high to trigger a detonation wave.

The boundary between these two modes is referred to as the strong ignition limit. Meyer and Oppenheim (1971) showed that the demarcation line between the two regimes is associated with a critical value of the gradient of the induction time with respect to temperature at constant initial pressure. At higher temperatures, the induction time is less sensitive to temperature variation and it is too short compared to the characteristic time for transport phenomena so that the latter do not influence the ignition process. In this case, the ignition takes place at the same time throughout the cross-section of the tube: it is the strong ignition regime. On the other hand, if the gradient of the induction time with respect to temperature becomes larger, the spatial non-uniformity in temperature after the shock leads to the formation of small distinct reaction centers so that the rate of heat released across the tube cross-section is too small to generate a significant pressure pulse. Since the induction time is longer, transport phenomena have a great influence on the process and small flame kernels are created: it is the mild ignition regime. Meyer and Oppenheim (1971) found a limiting value for a stoichiometric hydrogen-oxygen mixture:

$$\left(\frac{\partial \tau}{\partial T}\right)_P = -2\ \mu\mathrm{s} \cdot \mathrm{K}^{-1} \tag{1}$$

where τ is the induction time, T the temperature and P the pressure.

A third ignition regime was revealed by Gelfand et al. (1995) which is characterized by high pressure spikes behind the reflected shock wave. This regime is referred to as transient regime. For a given mixture, the values of the Mach numbers corresponding to this ignition mode fall in the range between the Mach numbers for mild and strong ignition. This range was found to expand when approaching the concentration limits. Gelfand et al. (2000) observed these high pressure spikes behind the reflected shock wave in the case of a wedge reflector. The high pressure spikes are due to a shock wave propagating in the direction of the reflector apex. They suggested that an explosion process, like detonation initiation for example, was at the origin of this wave.

4.3 Characteristic features of ignition by shock focusing

The critical incident shock Mach number for self-ignition depends on the mixture composition and the type of reflecting surface. The dependence of this critical Mach number on the fuel content has a characteristic U-shape. Moreover, the type of ignition regime depends on the mixture composition and the incident shock wave Mach number. For mild ignition, the reflected shock wave amplification (after ignition) does not depend on the mixture composition and the type of reflector, but depends only on the incident shock strength. However, for transient and strong ignition, the amplification depends on the mixture composition (Gelfand et al., 1995). This is expected, as the properties of the detonation or quasi-detonation wave overtaking the reflected shock wave are mixture-dependent.

The pressure profile behind the reflected shock wave is of course different depending on the ignition type. Borisov et al. (1990) and Gelfand et al. (2000) underlined the slow pressure rise along the reflector axis in the case of mild ignition in both hydrogen-air and hydrocarbon-air mixtures. This phenomenon is characteristic of a combustible mixture. In the case of an inert mixture, the pressure after the reflected wave remains constant. However, in the case of mild ignition, the creation of reaction centers slowly elevates the pressure to values much higher than the reflected wave pressure. The strong ignition case is characterized by a higher pressure peak than the expected reflected wave pressure.

Borisov et al. (1990) proved the existence of an optimum radius of curvature of the reflecting surface for self-ignition. For radii of curvature greater than the tube radius, the ignitability of the mixture was about the same as in the flat endplate case. As the radius of curvature decreased, the magnitude of igniting shock waves dropped dramatically before increasing again. The optimum radius of curvature corresponded to one tube radius. Its existence is believed to be due to weaker collapsing of reflected shock waves when the radius of curvature is large and to smaller volumes of hot mixture near the focus when the radius of curvature is small, giving a less intense ignition and motion of the shocked gas, and hence leading to longer times of flame spread.

4.4 Ignition location

Borisov et al. (1990) confirmed with Schlieren images that ignition was taking place in the case of cylindrical or spherical reflectors at the site and instant of collision of the reflected shock waves from the curved surface, i.e. at the gasdynamic focus. Pressure and radiation measurements showed that the maximum pressure and temperature values coincide in time and space. Similarly, Gelfand et al. (2000) noticed that the gasdynamic focus was always one of the reaction centers created in the case of mild ignition in a parabolic reflector. In the case of strong ignition for a parabolic reflector, detonation initiation coincided with the merging of the two diffracted shock waves on the reflector axis at the gasdynamic focus.

Wedge reflectors have a gasdynamic focus which is located at the wedge apex. The location of strong ignition is therefore located at the apex, as verified by Chan et al. (1990) and Gelfand et al. (2000). The creation of a flame kernel in the case of mild ignition also occurs at the apex, but flame kernels can also be created behind the multiple reflected shock fronts (Chan et al., 1990).

Gelfand et al. (2000) also showed that the absence of detonation initiation inside the reflector cavity did not exclude the possibility of detonation initiation outside the reflector cavity. The reaction centers characteristic of mild ignition can collapse outside the cavity to form a self-sustaining detonation wave. The distance from the apex L^* at which detonation initiation occurs was studied for a 90° wedge and a semi-cylinder. The distance L^* is closely linked to the kind of ignition regime that is obtained. For strong ignition, the value of L^* is zero as detonation initiation takes place at the reflector apex. For transient ignition, detonation initiation was observed to happen not more than 2 tube diameters away from the apex. Transient ignition is characterized by a system of weak bow shocks behind the reflected shock wave, some of these weak shocks being followed by burning of the mixture. It is the collision of these weak bow shocks on the axis that will trigger the formation of the detonation wave. In the mild ignition case, the distance increases with decreasing incident

shock Mach number. There is development of turbulent combustion zones in the vicinity of the tube walls behind the reflected shock wave. In this case, detonation initiation is due to the propagation of a complicated shape flame front in the flowfield behind the reflected shock wave.

4.5 Effect of reflection type on detonation initiation

The type of reflection is dictated by the geometry of the reflector and the intensity of the incident shock wave Mach number. Depending on the values of the Mach number and the slope of the reflector when the shock enters the cavity, either a regular or a Mach reflection is obtained (Ben-Dor, 1992). As the incident shock wave enters the cavity, a system of diffracted shocks propagate towards the centerline of the reflector. These diffracted shocks form two Mach configurations with the reflected shock, whose collision is responsible for focusing. Bartenev et al. (2000) confirmed the key-role of triple-point interaction for shock focusing, by observing detonation initiation at the focus of a deep parabolic reflector generating a type C reflection as described by Izumi et al. (1994).

For wedge reflectors, the type of reflection determines the initiating zone size and intensity. For regular reflection, ignition takes place exactly at the apex of the wedge. However, for Mach reflection, ignition happens in a small region located between the apex and the location of the second triple point collision. Numerical calculations by Bartenev et al. (2000) indicate that the behavior of the maximum temperature depends on the type of reflection. In the case of regular reflection, the maximum temperature was found to be independent of the size of the reflector; however, in the case of Mach reflection, the maximum temperature increased with the size of the wedge. Chan et al. (1990) carried out experiments with a 90° wedge at different orientations with respect to the flow. The experiments showed that the critical shock strength for ignition is very sensitive to the orientation of the wedge. The highest shock strength was needed when one face of the wedge was perpendicular to the flow whereas the lowest shock strength needed was when the faces of the wedge were at 45° with the tube centerline. Subsequent numerical calculations showed that as the angle decreases, one of the Mach stems disappears to be replaced by a regular reflection, while the other Mach stem becomes much wider. They explained that the resulting effect of having a regular reflection on one side and a wide Mach stem on the other side is to shift the point of collision between the waves (gasdynamic focus) away from the corner, thus reducing the focusing effect.

The crucial role of shock reflection type was also pointed out by Teodorczyk et al. (1988) for the propagation mechanism of quasi-detonations. A quasi-detonation propagating through an array of obstacles was observed to partly fail when diffracting over an obstacle. The diffracted wave hit the wall to form a regular reflection, before a transition to Mach reflection leading to re-initiation was observed. It is not clear whether this re-initiation process was caused by shock heating or by turbulent mixing at the vortex associated with the shear layer of the triple point.

4.6 Effect of scale

The consideration of shock focusing in a reactive medium introduces lengthscales associated with the kinetics of the mixture. No self-similar behavior is expected like in the inert case, and the results are scale-dependent.

Indeed, the critical conditions for ignition depend on the size of the reflector. Chan et al. (1990) and Bartenev et al. (2000) found the critical incident shock Mach number to decrease with increasing reflector size for a 90° wedge, being approximately inversely proportional to the linear size of the wedge. Bartenev et al. (2000) distinguished two cases for the maximum temperature variation with scale depending on the type of reflection obtained. However, an energy balance analysis showed that these two different cases result in similar effects on the critical Mach number.

The initial pressure of the mixture also has some influence on the critical conditions for ignition. Chan et al. (1990) showed that the critical conditions for both ignition and detonation initiation decrease with increasing initial pressure. At higher pressures, the deflagration regime was found to disappear as the critical conditions for both ignition and detonation onset become identical.

A diagram classifying the different regimes (inert, mild and strong) at shock wave focusing was proposed by Bartenev et al. (2000). This diagram plots the Mach number versus the governing parameters, such as initial pressure, reflector linear size and mixture sensitivity. This diagram is however quite qualitative as the boundaries between the different regimes cannot be accurately determined.

Mixture	Conditions	Reflector	Reference
$2H_2$+O_2	$P_{ref} = 0.23 - 1.96$ atm $T_{ref} = 900 - 1350$ K $M = 2.3 - 2.9$	flat	Meyer and Oppenheim (1971)
C_2H_4+$2O_2$ C_3H_8+$5O_2$	$P_0 = 30 - 200$ Torr $M = 1.6 - 4$	semi-cylinder (R=15, 29, 50 mm) 45° cone	Borisov et al. (1990)
lean H_2/air	$P_0 = 0.16 - 0.3$ bar $M = 2.3 - 2.9$	wedge (53° and 90°)	Medvedev et al. (1999)
15% H_2+85% air	$P_0 = 26.4 - 40$ kPa $M = 2.3 - 2.9$	parabola (y=0.11x^2) semi-cylinder (R=27 mm) wedge (53° and 90°)	Gelfand et al. (2000)
$2H_2$+O_2	$P_0 = 40 - 140$ Torr $M = 1.6 - 2.7$	90° wedge variable orientation	Chan et al. (1990)

Table 2: Summary of shock focusing studies in combustible mixture. P_0 is the initial pressure, T_0 the initial temperature, P_{ref} the reflected pressure, T_{ref} the reflected temperature and M the incident shock wave Mach number.

A summary of the different studies carried out on shock focusing in combustible mixtures is presented in Table 2. The different cases explored, including mixture, initial conditions, incident shock wave Mach number, reflector type and reference are displayed.

5 Conclusion

Pressure and temperature amplifications depend on the type of reflection. Type C reflection generates a higher pressure peak at shock focusing, however followed by a strong expansion wave than type A or B. Detonation initiation by shock focusing has been demonstrated by previous researchers. Ignition thresholds in terms of incident shock Mach number are found to depend on reflector type, mixture composition, and scale (size of the reflector). Further experiments are needed to develop predictive models of detonation initiation by shock focusing over a wider range of situations.

References

Bartenev, A. M., S. V. Khomik, B. E. Gelfand, H. Grönig, and H. Olivier (2000). Effect of reflection type on detonation initiation at shock-wave focusing. Shock Waves, Vol. 10, pp. 205–215. 16, 17

Ben-Dor, G. (1992). Shock wave reflection phenomena. Springer-Verlag New York, 1992. 16

Borisov, A. A., V. M. Zamanskii, V. V. Kozenkov, V. V. Lisyanskii, G. I. Skachkov, K. Y. Troshin, and B. E. Gelfand (1990). Ignition of gaseous combustible mixtures in focused shock waves. Current Topics in Shock Waves, AIP Conference Proceedings, Vol. 208, 1990. 15, 17

Brown, C. J. and G. O. Thomas (2000). Experimental studies of ignition and transition to detonation induced by the reflection and diffraction of shock waves. Shock Waves, Vol. 10, pp. 23–32, 2000. 13

Chan, C. K. (1995). Collision of a shock wave with obstacles in a combustible mixture. Combustion and Flame, Vol. 100, pp. 341–348, 1995. 13

Chan, C. K., D. Lau, P. A. Thibault, and J. D. Penrose (1990). Ignition and detonation initiation by shock focusing. Current Topics in Shock Waves, AIP Conference Proceedings, Vol. 208, 1990. 15, 16, 17

Gelfand, B. E., S. V. Khomik, A. M. Bartenev, S. P. Medvedev, H. Grönig, and H. Olivier (2000). Detonation and deflagration initiation at the focusing of shock waves in a combustible mixture. Shock Waves, Vol. 10, pp. 197–204, 2000. 14, 15, 17

Gelfand, B. E., S. V. Khomik, S. P. Medvedev, A. N. Polenov, A. M. Bartenev, and W. Breitung (1995). Self-ignition of combustible mixtures behind shock waves reflected at the non-flat surfaces at high initial pressures. Book of abstracts, Proceedings of the 20th International Sympsium on Shock Waves, Pasadena, California, p. 251, 1995. 14

Holl, R. and H. Grönig (1983). Focusing of weak blast waves. Proceedings of the 14th Internation Symposium on Shock Tubes and Waves, Sydney, Australia, pp. 563–568, 1983. 6, 7

Izumi, K., S. Aso, and M. Nishida (1994). Experimental and computational studies focusing processes of shock waves reflected from parabolic reflectors. Shock Waves, Vol. 3, pp. 213–222, 1994. 3, 5, 8, 9, 16

Kishige, H., K. Teshima, and M. Nishida (1991). Focusing of shock waves reflected from an axisymmetrically parabolic wall. Proceedings of the 18th International Symposium on Shock Waves, Sendai, Japan, Vol. 1, pp. 341–345, 1991. 6, 7, 8

Liang, S. M., C. S. Wu, F. M. Yu, and L. N. Wu (1995). Numerical simulation of shock wave focusing over parabolic reflectors. Shock Waves, Vol. 5, pp. 139–148, 1995. 6, 7

Liang, S. M., L. N. Wu, and R. L. Hsu (1999). Numerical investigation of axisymmetric shock wave focusing over paraboloidal reflectors. Shock Waves, Vol. 9, pp. 367–379, 1999. 5, 8

Medvedev, S. P., S. V. Khomik, and B. E. Gelfand (1999). Experimental evidence for detonation of lean hydrogen-air mixtures induced by shock focusing. Proceedings of the 17th ICDERS, Heidelberg, Germany, 1999. 17

Medvedev, S. P., S. V. Khomik, A. N. Polenov, and B. E. Gelfand (1995). Experimental evidences on peak temperature at the shock focusing. Book of abstracts, Proceedings of the 20th International Sympsium on Shock Waves, Pasadena, California, pp. 131–132, 1995. 7

Meyer, J. W. and A. K. Oppenheim (1971). On the shock-induced ignition of explosive gases. Proceedings of the 13th International Symposium on Combustion, The Combustion Institute, Pittsburgh, pp. 1153–1164, 1971. 14, 17

Milton, B. E. (1989). The focusing of shock waves in two-dimensional and axi-symmetric ducts. Proceedings of the International Workshop on Shock Wave Focusing, Sendai, Japan, March 22-23, 1989, pp. 155–191. 4, 5, 8

Nishida, M. (1989). Focusing of reflected shock waves. Proceedings of the International Workshop on Shock Wave Focusing, Sendai, Japan, March 22-23, 1989, pp. 140–153. 6, 7

Nishida, M., T. Nakagawa, and Y. Kikuyama (1986). Focusing of reflected shock waves. Transactions of the Japanese Society for Aeronautical and Space Sciences, Vol. 28, Nr. 82, pp. 209–217, 1986. 6, 7

Perry, R. W. and A. Kantrowitz (1951). The production and stability of converging shock waves. Journal of Applied Physics, Vol. 22, Nr. 7, pp. 878–886, 1951. 4

Quirk, J. J. (1998). AMRITA: A computational facility (for CFD modelling). *Lecture series - von Karman Institute for Fluid Dynamics 3*, D1–D72. 8

Sturtevant, B. (1989). The physics of shock focusing in the context of extracorporeal shock wave lithotripsy. Proceedings of the International Workshop on Shock Wave Focusing, Sendai, Japan, March 22-23, 1989, pp. 39–64. 6

Sturtevant, B. and V. A. Kulkarny (1976). The focusing of weak shock waves. Journal of Fluid Mechanics, Vol. 73, pp. 651–671, 1976. 3, 4, 6

Teodorczyk, A., J. H. S. Lee, and R. Knystautas (1988). Propagation mechanism of quasi-detonations. Proceedings of the 22nd International Symposium on Combustion, The Combustion Institute, Pittsburgh, pp. 1723–1731, 1988. 16